

# Modeling of Surface Tension in Fluidic MEMS Using the Level-Set Method

Koji TAKAHASHI

Kyushu University, Department of Aeronautics and Astronautics,  
Fukuoka 812-8581, JAPAN, takahashi@aero.kyushu-u.ac.jp

## ABSTRACT

A new numerical scheme for fluidic MEMS with gas and liquid mixture is developed in order to improve bubble or droplet-based microsystems. Key of the scheme for gas liquid two-phase flow is the modeling of surface tension force on the extremely thin interface between gas and liquid. This new scheme is successfully applied to simulate the thermocapillary motion of bubble in a microchannel by calculating the surface distribution accurately. Obtained results show good agreements with experimental data qualitatively. Several numerical assumptions required for micro fluidic systems especially near the channel wall are explained and differences with the conventional scheme are also discussed.

**Keywords:** CFD, Gas Liquid Interface, Microchannel, Surface Tension, Contact Angle

## 1 INTRODUCTION

Recently fluids are frequently used as major working element in a wide variety of micro systems; biochemistry, ink jet printer, heat exchanger, optical switch, and so on. So far such fluidic MEMS have been only treated for demonstration whether its operation principle works or not. However, it should be time to apply numerical simulation technique to improve and even to design the microfluidic components such as valve, pump, mixer, and so on. The single liquid flow or liquid/liquid flow has little difficulty to treat by CFD technique because of its low Reynolds number. However, the gas/liquid two-phase flow is difficult to simulate by CFD even in a macro system due to the difference of governing equations between liquid and gas when we use the Euler method. The Lagrange methods treat them separately but cannot be applied when the coalescence or fragmentation of each phase occurs. So that only the Euler method is treated and discussed in this paper.

One of the newest schemes for gas/liquid two-phase flow is C-CUP [1-3] using Level-Set method [4-6] and CSF [7] model. This combination works pretty well to simulate the macroscopic fluid system. However, many other difficulties can appear for further miniaturized systems in the order of less than  $100\mu\text{m}$ . Because the surface tension

becomes the most dominant mechanical effect in the miniaturized systems with bubble or droplet, enough attention should be paid in the discrete scheme for numerical analysis. Other effects such as electric double layer are also enough huge to consider carefully. But this paper does not treat them because my purpose is neither to choose material nor to understand electrical operation.

Because there is no perfect numerical scheme for the gas/liquid two-phase flow especially for fluidic MEMS, it is intended to develop a new reliable scheme by solving a bubble motion in a microchannel as a test bench. A bubble or droplet can be driven in a microchannel due to the thermocapillary force or surface tension imbalance [8-10]. This has been experimentally tested using temperature control by micro heaters on microchannel fabricated by MEMS technology as seen in Fig. 1. Comparing with the observed feature of bubble motion, several assumptions of fluidic parameter are employed. Finally reasonable modeling of surface tension is established and successful simulation of bubble driven by surface tension is performed.

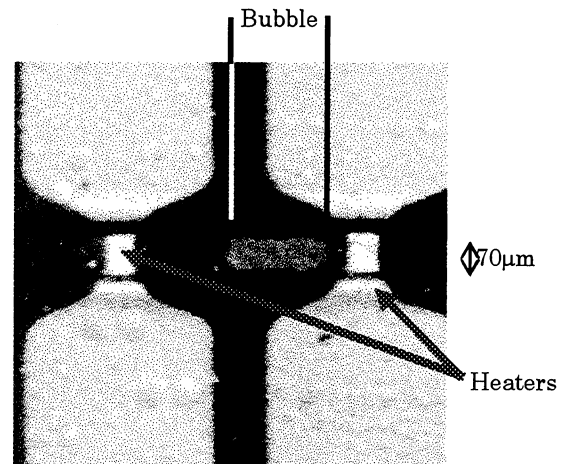


Fig. 1 Bubble migration in a microchannel driven by surface tension imbalance that is controlled thermally by the microheaters.

## 2 NUMERICAL SCHEME

For both gas and liquid, the same equations of compressible fluid is used in a two dimensional cylindrical

coordinate, where liquid is treated as a compressible fluid of extremely large sound velocity. The governing equations are written as the non-conservative form of the CIP method.

$$\begin{aligned} \frac{\partial \rho}{\partial t} + (\mathbf{u} \cdot \nabla) \rho &= -\rho \nabla \cdot \mathbf{u} \\ \frac{\partial \mathbf{u}}{\partial t} + (\mathbf{u} \cdot \nabla) \mathbf{u} &= \frac{1}{\rho} (-\nabla p + \mu \nabla^2 \mathbf{u} + \sigma \kappa \delta(L) \mathbf{n}) \\ \frac{\partial p}{\partial t} + (\mathbf{u} \cdot \nabla) p &= -\rho C^2 \nabla \cdot \mathbf{u} \end{aligned} \quad (1)$$

The Tait equation is used as the equation of state for a liquid,

$$\frac{p + Aw}{p_\infty + Aw} = \left( \frac{\rho}{\rho_\infty} \right)^{\eta_l} \quad (2)$$

where  $Aw$  is 294[MPa] and  $\eta_l$  is 7.14 for water. Gas phase is assumed to the perfect gas. The sound velocity is led from each equation of state as,

$$C_l = \sqrt{\frac{\eta_l (p_\infty + Aw)}{\rho_\infty} \left( \frac{\rho}{\rho_\infty} \right)^{\eta_l - 1}} \quad \text{for liquid} \quad (3)$$

$$C_a = \sqrt{\frac{\gamma_a p}{\rho}} \quad \text{for gas} \quad (4)$$

In order to capture the gas-liquid interface in the fixed grid, the Level-Set method is known to be useful. The phase of liquid and gas is indexed by the Level-Set function  $\phi$  as follows.

$$\phi(L) = \begin{cases} L > 0 & : \text{liquid} \\ L < 0 & : \text{gas} \\ L = 0 & : \text{interface} \end{cases} \quad (5)$$

where  $L$  is the length from the interface. In order to stabilize the numerical calculation on the interface ( $\phi=0$ ), transition region of a finite thickness ( $2\alpha$ ) is introduced by smoothing the density  $\rho$  as follows:

$$\rho(\phi) = \begin{cases} \rho_l & \phi > \alpha \\ \rho_a & \phi < -\alpha \\ \bar{\rho} + \Delta \rho \sin(\pi \phi / (2\alpha)) & -\alpha \leq \phi \leq \alpha \end{cases} \quad (6)$$

Smoothing of viscosity coefficient is performed in the same manner. Surface tension is treated by CSF model, which imposes the tension force on the transition region as the converted volume force  $F_{sv}$  (Fig. 2). Simulation of the

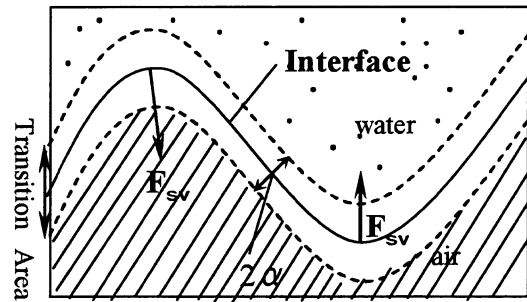


Fig.2 Transition area and surface tension model on the water-air interface

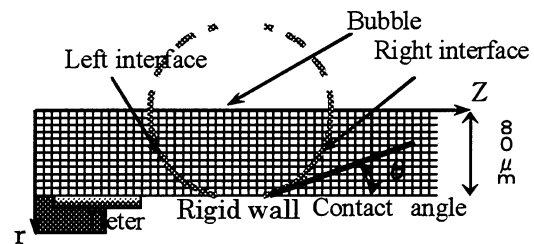


Fig.3 Computational grid and initial condition for a bubble in a microchannel

bubble motion in a circular microchannel of 80 $\mu\text{m}$ -radius is performed by using square grid of 2 $\mu\text{m}$  pitch in axisymmetric coordinate as explained in Fig. 3. The initial density of gas is 1 $\text{kg}/\text{m}^3$  and that of liquid 1000 $\text{kg}/\text{m}^3$ . The initial pressure of gas in bubble  $P_{in}$  is defined by the Young-Laplace equation

$$P_{in} - P_{out} = \frac{2\sigma}{R} \quad (7)$$

where  $P_{out}$  is set to atmospheric pressure.  $R$  is obtained initially from the contact angle as mentioned later. The surface tension  $\sigma$  is dependent on temperature there which is assumed to be 20 $^\circ\text{C}$  before starting and 100 $^\circ\text{C}$  after that in order to focus on the surface motion analysis.

Slip condition is a critical issue for microchannel calculation. From the experiments in Fig.1, liquid microlayer is always observed between migrating bubble and channel wall. The hydrophobic surface completely prevents bubble motion. This means that any simulation without liquid microlayer would not give realistic result. However, the microlayer is strongly dependent on material property. For example, its thickness is decided by the disjoining pressure and its mobility is by viscosity, wettability, and so on. Their physical understanding is far from satisfaction. This is why this paper imposes slip condition with constant contact angle in place of the presence of microlayer with non-slip condition. In other words, a finite thickness of fluid near channel wall is

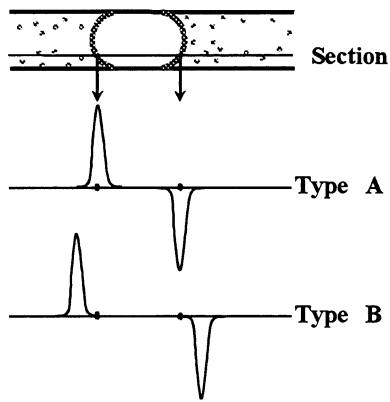


Fig.4 Comparison of surface tension models of conventional scheme (Type A) and new one (Type B) around a bubble in microchannel.

ignored and both of gas and liquid are assumed to slip on that layer as a first step of simulation modeling

At some preliminary calculations, there are found several problems for the Level-Set/CSF scheme for microscale liquid/gas interface simulation. In order to obtain converging results, a new method to treat the surface tension is used. As seen in Fig. 4, the surface tension force in the region of  $0 < \phi < 2\alpha$  (Type B) is newly imposed in place of the existing way of  $-\alpha < \phi < +\alpha$  (Type A). This is because Type A causes unusual acceleration of the transition region near gas phase due to its much smaller density than liquid and such unusual acceleration at several grids results in large oscillation and finally in numerical divergence. Even when the initial condition is set to satisfy Eq.7, unavoidable tiny numerical errors due to discrete grid position, etc., yield large imbalance of force that causes oscillations of bubble surface. Practical calculation is made to start after initial 1000 steps for the viscosity-induced decay of such oscillation.

Contact angle  $\theta$  is another possible source of numerical error. The condition of constant contact angle usually define the Level-Set function  $\phi$  as

$$\frac{\nabla\phi}{|\nabla\phi|} = \mathbf{t} \cos\theta + \mathbf{n} \sin\theta \quad (8)$$

where  $\mathbf{t}$  is unit vector tangential to the solid wall and  $\mathbf{n}$  is normal one. This equation means the gas/liquid interface on channel wall is a straight line that causes numerical error for the interface curvature. Here two types of extrapolation of bubble interface are tested as illustrated in Fig. 5, where old scheme is the usual method and the other one uses a curve fitting for extrapolation of bubble interface as to coincide with the contact angle. Figure 6 shows the comparison of obtained surface tension distribution indicating that the conventional scheme gives unphysical

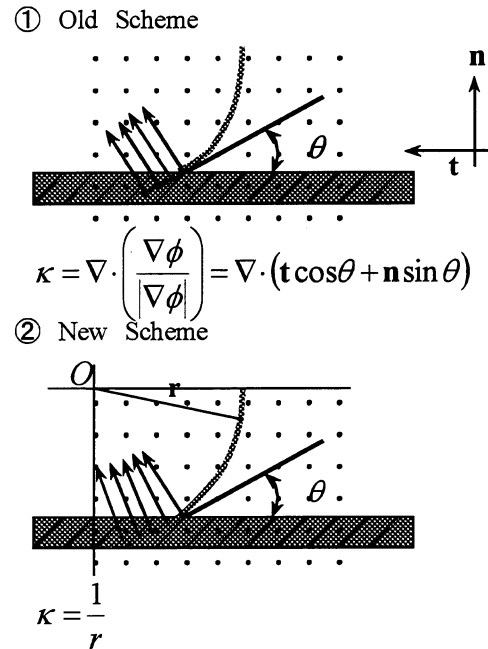


Fig.5 Extrapolation of interface and boundary conditions for constant contact angle

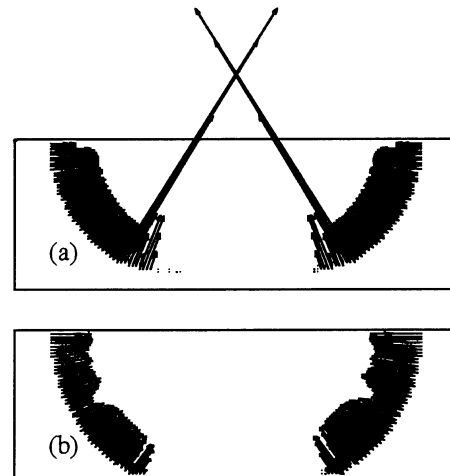


Fig.6 Comparison of distributions of surface tension obtained by using conventional (a) and new (b) schemes of the contact angle.

value while the extrapolation of bubble interface by a curve of  $k=1/r$  yield a acceptable result.

### 3 RESULTS AND DISCUSSIONS

Using the above-proposed updates for simulation of gas/liquid interface, thermally-driven bubble in microchannel is numerically analyzed. Figure 7 shows profiles of bubble interface, all of which keep their

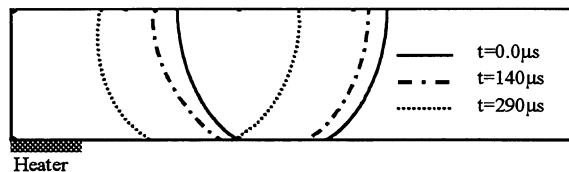


Fig.7 Calculated bubble interface profile in a microchannel.

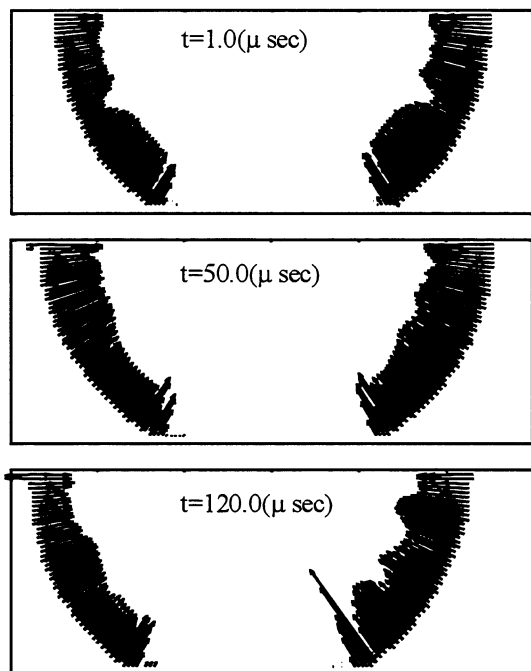


Fig.8 Surface tension distribution on bubble interface due to the artificial temperature imbalance.

spherical shape due to the enhanced surface tension effect in microchannel. Also the bubble is not of constant velocity but accelerated. This result is consistent with the preliminary experiments and is thought due to liquid momentum. The obtained quantitative velocity is different from experimental data probably because of the incorrect temperature assumption and full-slip condition.

The distribution of surface tension is shown in Fig. 8. The large tension seen in the near-wall region at  $t=120\mu\text{s}$  should be paid attention and this phenomenon can be explained from the temporary presence of large curvature there due to some mismatch between invariable contact interface and other deformable bubble surface. In other words, the large surface tension near the channel wall works as the restitution force to keep the bubble shape.

From the calculated pressure profiles that are not shown here, the mechanism of thermally-driven bubble is understood. The surface tension imbalance on bubble surfaces makes a difference of pressure gradient in both sides of liquid, which causes liquid motion resulting in bubble migration. Other calculations are also performed without keeping contact angle or with changing slip condition. Their results will be investigated in other paper but anyway the above-proposed numerical scheme was found to give the best results for gas/liquid interface in a microchannel.

## ACKNOWLEDGMENT

This work was partly supported by the Grant-in-Aid for Scientific Research from Ministry of Education, Culture, Sports, Science and Technology (No. 14702029). The author would like to thank Mr. Kou Koga, Dr. Ryoji Doihara, Mr. Koichiro Yoshino and Prof. Kunihito Nagayama for their numerical and experimental work and helpful discussion.

## REFERENCES

- [1] T. Yabe and P. Y. Wang, *J. Phys. Soc. Jpn*, **60**, pp.2105, 1991.
- [2] T. Yabe and P. Y. Wang, *J. Phys. Soc. Jpn*, **62**, pp.2537, 1993.
- [3] R. Doihara and K. Takahashi, *JSME Int. J, Ser.B*, **44**, pp.238, 2001.
- [4] M. Sussman, P. Smereka and S. Osher, *J. Compt. Phys.*, **114**, pp.146, 1994.
- [5] S. Osher and J. A. Sethian, *J. Compt. Phys.*, **79**, pp.12, 1988.
- [6] W. Mulder, S. Osher and J. A. Sethian, *J. Compt. Phys.*, **100**, pp.209, 1992.
- [7] J. U. Brackbill, D. B. Kothe and C. Zemach, *J. Compt. Phys.*, **100**, pp.335, 1992.
- [8] K. Takahashi, J. G. Weng and C. L. Tien, *Microscale Thermophysical Engineering*, **3**, pp. 169, 1999
- [9] H. Togo, M. Sato and F. Shimokawa, *IEEE MEMS1999*, pp.418, 1999.
- [10] K. Takahashi, et al., *IEEE MEMS2001*, pp. 286, 2001.